NUMERICAL SIMULATION OF PULVERIZED COAL COMBUSTION AND EMISSION

C.F. Bender, R.H. Essenhigh[1], U. Ghia[2], and M.L. Mittal
Program for Computational Reactive Mechanics
Ohio Supercomputer Center, Columbus, OH 43212

Keywords: Turbulence, Particle Mixing, Fluid Flow for Combustion

1 Introduction

The development of accurate computer simulation tools for coal combustion and emission represents a complex task. Like combustion of other fuels, coal combustion has the coupling of: i) exothermic chemical reactions; ii) heat transfer; and iii) two phase fluid flow, but with added complexities due to particle pyrolysis, the internal burning of the particles, and formation of ash and slag. At present, there are a number of commercial codes (proprietary in nature) that have been developed and/or are in use for aid in boiler design and performance predictions. There are many programs in the academic institutions as well, like the programs at the University of Illinoi, Imperial College of London, the University of New Castle in Australia etc. The program at the Brigham Young University (BYU) has been the most successful. Many industries use this code. This program uses time averaged equations for fluid flow and 'engineering' rate equations for combustion and is suitable for use even on workstations. Essenhigh's group at The Ohio State University has developed a one-dimensional model of a coal flame to study the kinetics of coal combustion with focus on the reactivity aspects.

The proposed program at the Ohio Supercomputer Center is complementary to the BYU program. We propose to use high performance computing techniques for numerical simulation of pulverized coal combustion and emission with details of fluid mechanics, heat transfer, and reaction kinetics for combustion. The BYU program can give the directions and help to validate some of our results. Under this program, we also propose to make a comparative performance evaluation of different models/combination of models for pyrolysis, volatile combustion, and char oxidation. Unlike in other programs, we have started with the simulation of two phase fluid flow to study the turbulent mixing of the coal particles and the effect of particles on the flow.

Turbulent mixing of particles has been studied by many authors [Crowe et al. (1988)]. The majority of the reviewed studies have used flow models involving either the time-averaged properties of the turbulence, or have treated the turbulent flow as a random field. However, with the recent developments in the understanding of turbulent shear flows, it is being suggested that particle dispersion in free shear layers might be strongly dependent on the time scale of the large organized structures in the flow. Samimy and Lele (1990) have recently studied the particle motion in a temporally evolving compressible shear layer. All of these studies emphasize particle dispersion by an idealized fluid in simple geometries and do not account for viscosity and the effects of combustor geometry.

The purpose of the present study is to simulate the particle dispersion in a temporally and spatially evolving turbulent shear layer. To the best knowledge of the authors, this is the first study in which a direct numerical simulation of particle dispersion by a viscous turbulent flow field for a combustor type geometry is carried out. It is known that the presence of large number of

[1]The Ohio State University, Columbus, Ohio
[2]University of Cincinnati, Cincinnati, Ohio.

solid particles or liquid droplets in the turbulent flow modifies the turbulent structure [Elghobasi and Abou-Arab (1983)]. The present study will determine the flow conditions in the combustor as modified by the presence of large number of coal particles.

2 Mathematical modeling

The combustion chamber is represented as an axisymmetric sudden step-expansion geometry. An inert gas flow with swirl is considered. Particles of three different sizes are injected at three different radial and four different angular positions in the throat region. As the gas flows, the particles are dispersed in the combustion chamber by turbulence. Because of the large number of actual coal particles in the combustor region, the representation is confined to a statistical sample. Therefore, each of these sample particles characterize a 'parcel' of like numbers all having the same initial size, velocity, and temperature. In the present analysis, radiation is not included in the energy equation.

2.1 The gaseous phase

The fluid flow in the combustion chamber is represented mathematically by the time-dependent Navier-Stokes, equations expressed as a transport equation for the vorticity vector ω.

$$\frac{\partial \omega}{\partial t} + (\mathbf{V} \cdot \nabla)\omega = (\omega \cdot \nabla)\mathbf{V} - \frac{1}{Re}(\nabla \times \nabla \times \omega) - \nabla \times \mathbf{S}_p \tag{1}$$

where

$$\nabla \times \mathbf{V} = \omega \tag{2}$$

and $\mathbf{S}_p$ is the interfacial drag force resulting from the interaction between particles and medium.

The incompressibility constraint

$$\nabla \cdot \mathbf{V} = 0. \tag{3}$$

for the present case of axisymmetric flow involving only two spatial coordinates, defines a stream function ψ given by

$$\mathbf{V} = \nabla\psi \times \hat{e}_3 \tag{4}$$

where $\hat{e}_3$ is a unit vector parallel to x^3. The governing equation for ψ is then obtained using Eq.(2).

The energy equation in conservation form with S_T as the source term can be written as

$$\frac{\partial T}{\partial t} + \nabla \cdot (\mathbf{V}T) = \frac{1}{Pe}[\nabla \cdot (\kappa \nabla T)] + S_T \tag{5}$$

2.2 Particulate phase

Lagrangian equations are used to compute the motion and heating of each sample as it traverses the gas in the combustion chamber. The usual assumptions are employed to derive these equations. Assuming non-deformable spherical particles, with density much higher than that of the fluid, virtual mass force, pressure gradient force and Basset force are all neglected. Particle-particle interaction and other force fields such as gravity are also presently not included in the analysis. The governing equations for the particle in nondimensional form are written as:

$$\frac{d\mathbf{V}_p}{dt} = \frac{1 + 0.15 Re_p^{2/3}}{\gamma_\tau}(\mathbf{V}_f - \mathbf{V}_p) \tag{6}$$

where $Re_p = |\mathbf{V}_f - \mathbf{V}_p| \gamma_d Re$ and $\gamma_\tau = \tau_p/\tau_f = \gamma_\rho \gamma_d^2 (Re/18)$, the ratio of the aerodynamic response time and the time scale for large turbulent structures. Thus, γ_d characterizes the effectiveness of the large-scale structures for particles moving laterally in the mixing region. Further, $\gamma_\rho = \rho_p/\rho_f$ and $\gamma_d = d_p/d$. Here, d denotes diameter, and subscripts p and f designate particle and fluid, respectively.

The particle energy equation is given as:

$$\frac{m_p dh_p}{dt} + r_p(h_p - h_f) = \dot{Q} \tag{7}$$

The parameter $\dot{Q}$ is the gain or loss by convection or radiation with the gas phase.

Eqs. (1) and (6) are coupled through the term $\mathbf{S}_p$ given by

$$\mathbf{S}_p = \sum_n \frac{(1 + 0.15 Re_p^{2/3})\rho_p}{\gamma_\rho \gamma_d^2 (Re/18)\rho_f} \alpha^n (\mathbf{V}_f - \mathbf{V}_\mathbf{p}) \tag{8}$$

with $\alpha^n = \frac{N\pi}{6}\frac{d_p^3}{\Delta \mathbf{v}}$, N being the number of particles represented by the trajectory n and $\Delta\mathbf{v}$ is the computational cell volume.

2.3 Solution procedure

The analysis as well as the numerical solution procedure used to simulate the fluid flow follow the work of Osswald, et al. (1984). Writing the vorticity vector as

$$\omega = \omega^1(r,z)\vec{e}_1 + \omega^2(r,z)\vec{e}_2 + \omega^3(r,z)\vec{e}_3 \tag{9}$$

where ω^i are the contravariant components of vorticity and $\vec{e}_i$ are the covariant base vectors parallel to ξ^i coordinates, the governing equation for ω^3 in a generalized orthogonal curvilinear coordinate system (ξ^1, ξ^2, ξ^3) is derived.

$$\begin{aligned} &\sqrt{g}\frac{\partial \omega^3}{\partial t} + \frac{\partial}{\partial \xi^1}\left(\omega^3 \frac{\partial \psi}{\partial \xi^2}\right) - \frac{\partial}{\partial \xi^2}\left(\omega^3 \frac{\partial \psi}{\partial \xi^1}\right) \\ &= \frac{1}{Re}\left[\frac{\partial}{\partial \xi^1}\left(\frac{g_{22}}{\sqrt{g}}\frac{\partial}{\partial \xi^1}(g_{33}\omega^3)\right) + \frac{\partial}{\partial \xi^2}\left(\frac{g_{11}}{\sqrt{g}}\frac{\partial}{\partial \xi^2}(g_{33}\omega^3)\right)\right] \end{aligned} \tag{10}$$

g_{ii} are defined as

$$g_{ii} = \sum_{k=1}^{3} \left(\frac{\partial x^k}{\partial \xi^i}\right)\left(\frac{\partial x^k}{\partial \xi^i}\right). \tag{11}$$

with $g = g_{11}g_{22}g_{33}$ and $h_i = \sqrt{g_{ii}}$.

The stream function ψ is determined from

$$\frac{\partial}{\partial \xi^1}\left(\frac{g_{22}}{\sqrt{g}}\frac{\partial \psi}{\partial \xi^1}\right) + \frac{\partial}{\partial \xi^2}\left(\frac{g_{11}}{\sqrt{g}}\frac{\partial \psi}{\partial \xi^2}\right) = -\sqrt{g}\omega^3. \tag{12}$$

The azimuthal component of velocity v_ϕ gives the swirl velocity of the flow. The governing equation for v_ϕ is

$$\begin{aligned}
&\frac{\partial v_\phi}{\partial t}+\frac{1}{\sqrt{g}}\left[\frac{\partial}{\partial \xi^1}\left(\frac{\partial \psi}{\partial \xi^2}v_\phi\right)-\frac{\partial}{\partial \xi^2}\left(\frac{\partial \psi}{\partial \xi^1}v_\phi\right)\right]+\frac{v_x v_\phi}{h_1 h_3}\frac{\partial h_3}{\partial \xi^1}+\frac{v_r v_\phi}{h_2 h_3}\frac{\partial h_3}{\partial \xi^2}= \\
+&\ \frac{1}{Re}\times\frac{1}{\sqrt{g}}\left[\frac{\partial}{\partial \xi^1}\sqrt{\frac{g_{22}}{g_{11}}}g_{33}\frac{\partial}{\partial \xi^1}\left(\frac{v_\phi}{\sqrt{g_{33}}}\right)+\frac{\partial}{\partial \xi^2}\sqrt{\frac{g_{11}}{g_{22}}}g_{33}\frac{\partial}{\partial \xi^2}\left(\frac{v_\phi}{\sqrt{g_{33}}}\right)\right] \\
+&\ \frac{1}{Re}\left[\frac{1}{g_{11}}\frac{\partial\sqrt{g_{33}}}{\partial \xi^1}\frac{\partial}{\partial \xi^1}\left(\frac{v_\phi}{\sqrt{g_{33}}}\right)+\frac{1}{g_{22}}\frac{\partial\sqrt{g_{33}}}{\partial \xi^2}\frac{\partial}{\partial \xi^2}\left(\frac{v_\phi}{\sqrt{g_{33}}}\right)\right]-\frac{1}{\sqrt{g_{33}}}\frac{\partial p}{\partial \xi^3}
\end{aligned}\tag{13}$$

In the generalized orthogonal coordinate system, the energy equation (5) transforms as

$$\begin{aligned}
&\sqrt{g}\frac{\partial T}{\partial t}+\frac{\partial}{\partial \xi^1}\left(T\frac{\partial \psi}{\partial \xi^2}\right)-\frac{\partial}{\partial \xi^2}\left(T\frac{\partial \psi}{\partial \xi^1}\right) \\
&=\frac{1}{Pe}\left[\frac{\partial}{\partial \xi^1}\left(\frac{\sqrt{g}}{g_{11}}\frac{\partial}{\partial \xi^1}(\kappa T)\right)+\frac{\partial}{\partial \xi^2}\left(\frac{\sqrt{g}}{g_{22}}\frac{\partial}{\partial \xi^2}(\kappa T)\right)\right]+S_T\sqrt{g}
\end{aligned}\tag{14}$$

2.3.1 Boundary and initial conditions

At the radial boundaries, the flow conditions are derived from symmetry across the centerline and zero slip at the walls. The streamwise asymptotic forms of the governing equations (10-14) are solved to provide the inflow/outflow boundary conditions; this approach maintains consistency between the boundary values and the interior solution. The initial conditions correspond to a flow starting impulsively from rest.

2.3.2 Numerical mesh

An appropriate coordinate system is obtained by a conformal mapping of the sudden-expansion geometry to a uniform cross-section configuration. This mapping is further augmented by clustering/stretching transformations so as to provide resolution of the prevailing flow features and to provide for placing the inflow and outflow boundaries at upstream and downstream infinity, respectively.

2.3.3 Numerical solution

Starting from the initial state, the vorticity field is advanced using an alternating-direction implicit method. The corresponding stream-function distribution is obtained by a direct, fully implicit solution of the elliptic stream function equation. The time evolution of the flow field is pursued as long as desired. All spatial derivatives are discretized using second-order accurate central differences. Care is taken to ensure proper grid-point placement so as to obtain satisfactory results.

3 Results and discussion

The numerical computations have been performed at the Ohio Supercomputer Center using the CRAY Y-MP 8/864 supercomputer. Figure 1 shows the geometry and the grid distribution for the sudden axisymmetric step-expansion geometry. A grid of 635 points is used in the axial direction and 132 points in the radial direction, with $Re = 1.0 \times 10^3$ and time step $\Delta t = 2.0 \times 10^{-6}$. Three values of γ_d, namely $\gamma_d = 10.0^{-5}, 20.0^{-5}, and 40.0^{-5}$ are considered to simulate the effect of particle size on mixing. Figures 2-4 show the instantaneous particle positions and vorticity contour lines at nondimensional time t = 0.695, 0.815, and 0.820. Only regions containing particles are shown. Initially, the entering particles move downstream in a rectilinear fashion with the fluid but then the fluid vorticity starts to affect their movement. The lighter particles start circulating first, with all particles eventually following suit. At later times, a rather interesting feature develops. As seen from their distribution overlaid on the vorticity field, the particles tend to be entrapped by the evolving large-scale vortex structure. This feature appears to be initiated in regions of reduced axial fluid velocity . At a later time, some of these particles move upstream while others move downstream at the upper periphery of the middle vortex structure; those in the region between two vortex structures move very rapidly towards the lower periphery of the downstream vortex.

The curves for temperature distribution are not shown here. The fluid temperature gives the thermal environment for the particles.

4 Conclusion

The numerical simulation of coal combustion is a challenging computational problem as it covers many different phenomena. The present effort represents a first step to provide a unified approach to the problem, using direct numerical simulation. This simulation has considered particle mixing in an adiabatic isothermal flow.

5 Future work

Work is in progress to study the combustion of single coal particle. This study needs the solution of the energy equation with radiation and the solution of the energy equation for particulate phase. Simultaneously, we are making parametric studies to determine the effect of swirl on particle dispersion and the effect of particle motion on the fluid flow.

References

[1] G. A. Osswald, K. N. Ghia, and U. Ghia, *AIAA Paper* 84-1584(1984)

[2] J. N. Chung and T. R. Troutt, *J. Fluid. Mech.* 186, 199-222 (1988)

[3] M. Samimy and S. K. Lele, *Phys. Fluids* (1990) To appear

[4] V.G. McDonnell and G. S. Samuelsen, *AIAA Paper* AIAA-91-0082 (1991)

[5] S.E. Elghobashi and T. W. Abou-Arab, *Phys. Fluids* 26, 931-938 (1983)

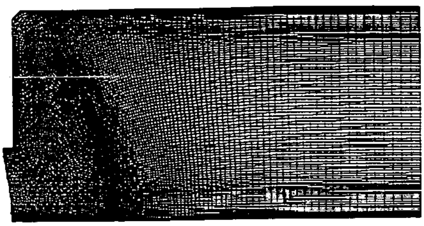

Typical Grid 635 x 132 Figure 1.

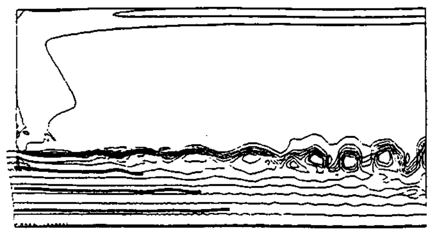

xo=-0.01, Re= 1000., Time= 0.825 xi= 2.06 Figure 2.

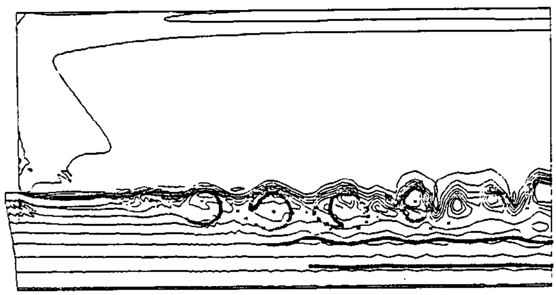

xo=-0.01, Re= 1000., Time= 0.820, xi= 2.06 Figure 3.

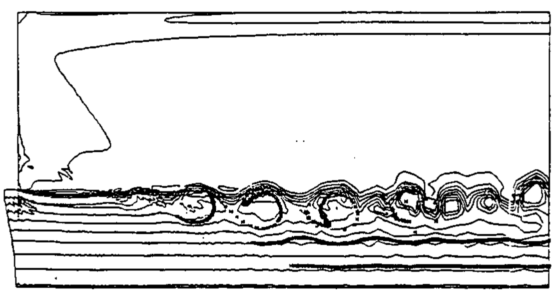

xo=-0.01, Re= 1000., Time= 0.815, xi= 2.06 Figure 4.